

1644

102
5/1/80

DR 1124

MARCH 1980

PPPL-1644

UC-20f

OBSERVATIONS OF GIANT RECOMBINATION
EDGES ON PLT TOKAMAK INDUCED BY
PARTICLE TRANSPORT

MASTER

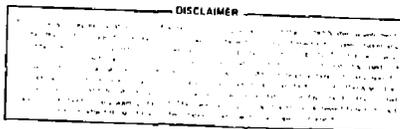
PLASMA PHYSICS
LABORATORY



DISTRIBUTION OF THIS DOCUMENT IS UNLIMITED

PRINCETON UNIVERSITY
PRINCETON, NEW JERSEY

This work was supported by the U. S. Department of Energy
Contract No. EY-76-C-02-3073. Reproduction, translation,
publication, use and disposal, in whole or in part, by or
for the United States Government is permitted.



Observations of Giant Recombination Edges on PLT
Tokamak Induced by Particle Transport

K. Brau, S. von Goeler, M. Bitter, R. D. Cowan, D. Eames, K. Hill,
N. Sauthoff, E. Silver, W. Stodiek
Plasma Physics Laboratory, Princeton University
Princeton, NJ 08544

ABSTRACT

In this paper we report on the observation of characteristic "steps" in the continuum spectrum of high temperature tokamak plasmas associated with recombination radiation from impurity ions. During special argon-seeded discharges on the Princeton Large Torus (PLT) tokamak the x-ray spectrum exhibited large enhancements over the bremsstrahlung continuum beginning with energies of 4.1 keV. This corresponds to the radiative capture of free electrons by hydrogen-like argon into the ground state of helium-like argon. The size of these edges increased to unexpectedly large values with minor radius (decreasing electron temperature), consistent with a departure of the hydrogen-like species from the predictions of corona equilibrium. Hence, the coronal equilibrium equations must be modified to

account for the radial transport of argon. A simple particle diffusion model is proposed, with the Ar XVIII radial profiles evaluated from the size of the recombination edges. For the case of moderate density ($\langle n_e \rangle \sim 3 \times 10^{13} \text{ cm}^{-3}$) and temperature [$T_e(0) \sim 1.5 \text{ keV}$] discharges the outward radial transport velocity is found to be approximately 10 m/sec.

INTRODUCTION

Continuum radiation from hot plasmas in the soft x-ray regime arises primarily from two atomic processes: bremsstrahlung and radiative recombination. For pure hydrogen plasmas with temperatures in the keV range, bremsstrahlung is the dominant process. When impurities (oxygen, iron) are present in sufficient concentrations, then recombination radiation may contribute the bulk of the continuum radiation. Measurements of the x-ray continuum of Tokamak plasmas showed in fact that the radiation intensity is too high to be accounted for solely on the basis of bremsstrahlung, and the enhancement of the x-ray continuum over bremsstrahlung was consequently attributed to recombination radiation from impurity ions.¹ This type of radiation is manifested in the spectrum as a series of continuum regions separated by steps, the continuum regions obeying the same exponential dependence on electron temperature as the bremsstrahlung, and the steps corresponding to the recombination of electrons into different energy levels of the impurity ions. Experimental confirmation of this theory rests largely on the observation of these recombination "edges." Yet because of the type and concentration of impurity ions normally present in Tokamak discharges and the restricted energy range of the detection system, such edges eluded observation and the presence of recombination radiation could only be inferred from the enhancement over the bremsstrahlung continuum.

This paper reports on the actual observation of a recombination edge during special argon-seeded discharges on the

PLT tokamak. The edge, which occurred at a photon energy of 4.1 keV (the ionization potential of helium-like argon) corresponds to the recombination of electrons with hydrogen-like argon ions into the ground level of the helium-like charge state. One would assume this edge to be most prominent in the central high temperature region of the plasma where the hydrogen-like species has its highest relative abundance under the assumption of coronal equilibrium. The experiment, on the contrary, showed giant recombination edges in spectra from the outer, colder regions of the discharge where the amount of hydrogen-like argon ought to be negligible. The size of these steps was unusually large, amounting in some cases to enhancements of the continuum by a factor of a thousand. In order to explain this large enhancement one must assume that hydrogen-like argon is not in a state of coronal equilibrium throughout the plasma but is being transported outward from the center of the discharge. Indeed, a state of coronal equilibrium exists only so long as the times characterizing atomic processes are much shorter than those associated with particle transport, while in the present case radiative recombination of hydrogen-like argon is a slow enough process that significant departures from coronal equilibrium are possible, assuming even moderate transport velocities.

The large recombination steps then, beyond giving an experimental confirmation of radiative recombination, ought to yield information about the radial transport velocity (or particle confinement time) of impurities in Tokamaks. Since

there are at present only few and often very debatable methods available to measure this transport, this aspect of our investigation has been extremely valuable. The observation of giant recombination edges thus has applications both in the fields of atomic physics and in controlled thermonuclear fusion research.

The remainder of this paper is divided into three parts. In the first section we describe the experimental setup used to detect soft x-ray radiation on PLT and present spectra taken during the special argon-seeded discharges. In the second part we review relevant radiative processes in the soft x-ray regime and discuss the predictions of the corona equilibrium model for the recombination edges. Finally, in the third section, we calculate the transport velocity and compare it to current estimates of ion particle confinement times.

A. Pulse height analysis system

The soft x-ray radiation (1-15 keV) on PLT is measured by the Pulse Height Analysis (PHA) system (Fig. 1). The primary function of this system is to provide information about the electron temperature profile and impurity content of the plasma. At its heart are four liquid nitrogen-cooled lithium-drifted silicon detectors. An incoming photon creates electron-hole pairs in the crystal in a number proportional to the photon energy; the resultant pulses are sorted according to their energies and counted by the pulse height analyzer to yield an energy spectrum. Since the photon flux varies by several orders

of magnitude over the emission spectrum, separate detectors are employed in the low and high energy regions. This allows one to optimize statistics and at the same time to avoid the problem of spurious "double pulses". Individual detector count rates are limited by a set of movable apertures and foils placed in front of the detectors.

During a PLT discharge data are taken in fourteen separate time groups for each of the detectors and are then processed by a PDP-10 computer. After correction for foil attenuation, count rate, geometry and detector efficiency, the spectra are overlapped into one spectrum. The analysis program then fits a third order polynomial to the continuum and computes the area under the impurity peaks. This process is repeated for several minor radii, and the resulting data are Abel inverted to obtain electron temperature and impurity profiles.

In Fig. 2 we present typical line integrated spectra obtained with the PHA during the argon-seeded discharges. There are two sets of data involving measurements taken on November 6, 1976 and September 20, 1978. One can see quite clearly various $K\alpha$ and $K\beta$ lines of argon and iron superimposed on the recombination continuum. Note also the giant recombination edges at $E = 4.1$ keV at outer radii, which for the 1976 spectra correspond to enhancements of 1000. Although argon levels (and thus the height of the 4.1 keV recombination edge) were not so high in the latter discharges, we have used this more complete set of data to calculate the radial transport velocity of argon.

2. Radiative Processes in the Soft X-ray Regime

A fairly complete description of the x-ray emission from hydrogen ions and impurities in the plasma may be found elsewhere in the literature.¹ Here we summarize conclusions of that discussion.

We first consider bremsstrahlung. For a Maxwellian plasma the power dW emitted per photon energy interval dk by bremsstrahlung is given by

$$\left(\frac{dW}{dk}\right)_{\text{brems.}} = 3 \times 10^{11} \frac{n_e \sum_i n_i Z_i^2}{10^{26} \text{ cm}^{-3}} \left(\frac{T_e}{\text{keV}}\right)^{-1/2} \bar{g}_{ff}(T_e, k) \exp(-k/T_e) \text{ sec}^{-1}$$

where n_e and n_p are the electron and ion densities, respectively, T_e the electron temperature, Z_i the positive ion charge, k the photon energy, and \bar{g}_{ff} the temperature-averaged Gaunt factor, normally taken equal to unity. The electron temperature is then found as the inverse of the slope in a semilogarithmic plot of the intensity dW/dk vs. photon energy. Strictly speaking, this procedure is valid only when applied to the Abel inverted spectra. One may nonetheless obtain a good approximation to the electron temperature directly from the raw spectra if one considers only the high energy region of the continuum where so-called "profile effects"¹ are less important.

Next we consider x-ray radiation that results when free electrons recombine into unoccupied energy levels of impurity ions. Again, for a Maxwellian plasma with ion density n_i of charge $Z_i - 1$, ground state ionization potential χ_i , and principal quantum number n , the x-ray intensity is given by

$$\left(\frac{dW}{dk}\right)_{\text{recomb.}} = 3 \times 10^{11} \text{ sec}^{-1} \frac{n_e \sum_i n_i z_i^2}{10^{26} \text{ cm}^{-3}} \left(\frac{T_e}{\text{keV}}\right)^{-1/2} \bar{g}_{\text{fb}}(T_e, k) \exp(-k/T_e)$$

$$\left[\frac{\xi}{n^3} \frac{\chi_i}{T_e} \exp \frac{\chi_i}{T_e} + \sum_{\nu=1}^{\infty} \frac{2\chi_H}{T_e} \exp \left(\frac{z_i^2}{(n+\nu)^3} \frac{\chi_H}{T_e} \right) \right]$$

where χ_H is the ionization potential of hydrogen, \bar{g}_{fb} the temperature averaged Gaunt factor for free-bound transitions, also taken equal to unity, and ξ is a statistical factor.² This equation may also be written in terms of the bremsstrahlung intensity as

$$\left(\frac{dW}{dk}\right)_{\text{recomb.}} = \left(\frac{dW}{dk}\right)_{\text{brems.}} (\gamma - 1)$$

where $(\gamma - 1)$ is given by the term in brackets multiplied by $(z_i/z_{\text{nuclear}})^2$. Expressed in this fashion, recombination radiation is seen to produce an effective "enhancement" over bremsstrahlung: i.e., the x-ray continuum is shifted upward by an amount proportional to $(\gamma - 1)$ without a change in slope. An x-ray spectrum in the presence of impurities will therefore exhibit a series of steps or edges, each corresponding to the recombination of electrons into a different energy level.

In the case of Ar XVIII the enhancement factor $(\gamma - 1)$ for the 4.1 keV recombination edge grows extremely large for temperatures less than 500 eV (Fig. 4). Normally one would not expect to see this edge at such low temperatures because the concentration of Ar XVIII is negligible if one assumes a state

of corona equilibrium (see below). Nevertheless, it is clear from Fig. 4 that only small departures of hydrogen-like argon from corona equilibrium are required to produce the observed giant recombination edges. We shall return to a more quantitative discussion of this effect in the next section.

Resonant line emission from impurity ions constitutes a third important source of radiation in the x-ray regime. There are two complementary processes that lead to line radiation. The first of these, collisional excitation, involves the excitation of an electron to a higher level by a free electron; a photon is emitted when the de-excited electron returns to its ground state. The second type, dielectronic recombination, is a three step process in which a free electron recombines to a high level of the ion, simultaneously exciting a bound electron to a higher level, and both emitting photons as they make the transition to the ground state. The radiation emitted in these processes is called $K\alpha$ if it involves a $1s-2p$ transition. Theoretical collisional excitation and dielectronic recombination cross sections for argon have been calculated by Merts, Cowan, and Magee² of LASL for electron temperatures in the range 200 to 2000 eV. The intensity of a $K\alpha$ line is proportional to the quantity $n_e n_{imp} \langle \sigma v \rangle_{total}$, where $\langle \sigma v \rangle_{total}$ represents the total dielectronic and collisional excitation cross section for the transition and involves some type of average over the charge state distribution. (Usually, corona equilibrium is assumed.) Abel inversion of the line-integrated $K\alpha$ emissivities then provides a simple method of determining

the local impurity concentration.

To determine the distribution of charge states in coronal equilibrium, we balance the processes of ionization and recombination

$$\frac{n_i}{n_{i-1}} = \frac{\langle \sigma v \rangle_i}{\alpha_i}$$

where $\langle \sigma v \rangle_i$ is the collisional ionization rate for ionization to the i^{th} charge state, and $\alpha_i = \alpha_{\text{rad}} + \alpha_{\text{diel}}$, is the total recombination rate of the i^{th} charge state. The distribution of charge states also enters into the computation of the effective enhancement factor γ_{eff} , defined as

$$\gamma_{\text{eff}} = \frac{\sum_i n_i Y_i}{\sum_i n_i}$$

The results of this calculation for argon are shown in Fig. 4, superimposed on the curves representing γ for individual charge states. It is clear from the graphs of γ_{eff} calculated both before and after the 4.1 keV recombination edge, which diverge only at $T_e \sim 800$ eV, that corona equilibrium cannot explain the observed giant recombination edges.

3. Calculation of the Radial Transport Velocity

The presence of giant recombination steps in the low temperature region of the discharge, a result which is in disagreement with the assumptions of corona equilibrium, indicates that an outward radial transport of argon must occur. The extent to which the equilibrium concentrations of the various charge

states of argon are affected by this transport may be determined in a qualitative manner from the collisional ionization and total recombination rates plotted in Figs. 5a and b.

Fig. 5b is the especially revealing graph. One sees that the recombination rates of highly-stripped argon (Ar XVII - Ar XIX) are significantly lower than those corresponding to species with partially filled L-shells. (This is simply a result of the reduced probability of dielectronic recombination for the energetically unfavorable K shell transitions.) Therefore, it is the highly-stripped species of argon with their relatively small recombination rates that may persist for times long enough to exhibit transport-induced departures from coronal equilibrium.

To calculate a transport rate for the hydrogen-like species of argon we employ a more general form of the corona equilibrium equations that is equivalent to a particle continuity equation including source terms:

$$\frac{\partial n_{17}}{\partial t} + \frac{1}{r} \frac{\partial}{\partial r} r D \frac{\partial n_{17}}{\partial r} =$$

$$n_e [n_{16} \langle \sigma v \rangle_{16} - n_{17} \langle \sigma v \rangle_{17} + n_{18} \alpha_{18} - n_{17} \alpha_{17}] .$$

Here n_i is the number density of the i^{th} charge state of argon, α_i and $\langle \sigma v \rangle_i$ the total recombination and ionization rates, respectively, of the i^{th} charge state, and D the diffusion coefficient. In general, a rigorous calculation of the diffusion process involves a coupled set of equations that includes all charge states of the impurity ion. For our purposes, however, this added

complexity is unnecessary.

A few terms may be discarded immediately from the diffusion equation. Experimentally, we find that the argon concentration reaches steady state after $t = 200$ ms, which allows us to take $\partial n_{17}/\partial t = 0$ at $t > 200$. Two of the source terms may also be neglected. For electron temperatures less than 800 eV the collisional ionization rate of Ar XVIII is much less than its radiative recombination rate. The term involving radiative recombination into the fully-stripped species of argon may also be ignored as this species is present only in negligible amounts throughout the plasma.

The remaining two source terms, $n_{16} \langle \sigma v \rangle_{16}$ and $n_{17} \alpha_{17}$, are calculated using some results from section two of this paper. An upper bound for the term $n_{16} \langle \sigma v \rangle_{16}$ may be estimated if the total argon impurity concentration is known (remember that the helium-like species of argon is not necessarily in corona equilibrium because of radial transport). There are two complementary procedures for obtaining n_{Ar}/n_e , one involving line radiation, the other, recombination radiation.

The first method, which makes use of the local K α line intensities for argon, has already been described in section two. The validity of this technique is limited by three factors: 1) uncertainties in the theoretically determined excitation and dielectronic recombination cross sections (estimated to be smaller than a factor of two), 2) departures from corona equilibrium leading to errors arising from the averaging of $\langle \sigma v \rangle_{total}$ over charge states; this introduces at most a factor of two uncertainty, and 3) the very strong temperature dependence of

$\langle \sigma v \rangle_{\text{total}}$ at low temperatures. In this case a temperature uncertainty in T_e of ten percent may lead to a factor of three error in the calculated argon concentration.

Because of the sensitivity to electron temperature variations it is more advantageous to obtain the argon concentration from the enhancement of the continuum spectrum over bremsstrahlung. According to the theory of recombination radiation the y-intercept of the Abel inverted energy spectrum is proportional to the quantity, $\sum_k n_k Y_k Z_{\text{eff},k}^2 / T_e^{1/2}$, where the index k refers to the different impurity species. If one extrapolates the central concentrations of titanium and the stainless steel elements as determined from K α lines to the region where the recombination edges occur and also makes use of spectroscopic estimates of the oxygen level, one finds that the contribution to the x-ray spectrum resulting from the radiative recombination of electrons with these elements is less than ten percent of the observed enhancement over bremsstrahlung. It is therefore reasonable to assume that the enhancement is produced almost entirely by the argon impurity. (The error introduced by neglecting recombinative enhancement from the other elements is in fact less than the uncertainty in the determination of the y-intercept.) The n_{Ar} profile obtained by this method is shown in Figure 6a.

Having established an upper bound for n_{16} (which is simply the total argon fraction n_{Ar}) we need to determine the Ar XVIII concentration, n_{17} , in order to establish which of the two source terms, $n_{16} \langle \sigma v \rangle_{16}$ and $n_{17} \alpha_{17}$, is dominant in the region of interest. The quantity, n_{17} , is obtained from the enhancement over bremsstrahlung at the 4.1 keV recombination edge. The x-ray

intensity at a photon energy, 4.1 keV, is approximately given by:

$$\left(\frac{dW}{dk}\right)_{E=4.1\text{keV}} = 3 \times 10^{11} \frac{n_i z_i^2}{T_e^{1/2}} \left(\frac{\chi_i}{T_e} + \sum_{\nu=1}^{\infty} \frac{2\chi_H}{T_e} \frac{z_i^2}{(\nu+1)^3} \exp\left\{ \frac{z_i^2 \chi_H}{T_e} \left[\frac{1}{(\nu+1)^2} - 1 \right] \right\} \right)$$

For $T_e \leq 1/5 \chi_i$, the terms in the summation are small compared to the first term, and the expression for n_{17} then reduces to a simple equality. In practice the x-ray intensity at 4.1 keV for the $r \geq 25$ cm spectra is complicated by the presence of a titanium K α line produced by x-ray fluorescence from a titanium shield mounted inside the PLT vacuum vessel and directly within the line of sight of the detector. The purpose of the shield was to enable discrimination between iron K α radiation emitted in the plasma and that produced by wall fluorescence. We have attempted to correct for this extra source of radiation by subtracting from the argon spectra typical Ti K α fluorescence lines measured during normal PLT discharges with comparable n_e and T_e . The Ti fluorescence spectra consist of large lines which protrude strongly over the continuum background, so that this correction has practically no effect on the continuum. The results of the calculation of the n_{17} profile are presented in Figure 6b.

We may now compare the contributions of the ionization and recombination source terms to the diffusion equation. Based on collisional ionization and radiative recombination rates supplied by R. D. Cowan,³ we find $n_{16} \langle \sigma v \rangle_{16} \langle n_{Ar} \rangle_{16} \leq 6 \times 10^{-5}$ (for $T_e \leq 500$ eV, $r = 25$ cm) and $n_{17} \alpha_{17} \sim 3 \times 10^{-3}$. Hence, the source term, $n_{16} \langle \sigma v \rangle_{16}$, may be ignored over the region of interest

where the recombination steps occur, and we need consider only the recombination term, $n_{17}\alpha_{17}$. (It may be noted briefly that the recombination rate of Ar XVIII is determined predominantly by radiative rather than by dielectronic recombination for electron temperature well below the 1s-2p excitation energy of 3.1 keV). Thus the source term is given by a simple and well established expression.

With the above approximations the diffusion equation reduces to the following simple formula

$$\frac{1}{r} \frac{\partial}{\partial r} (rD) \frac{\partial n_{17}}{\partial r} = -n_e n_{17} \alpha_{17} \quad .$$

The diffusion equation is seen to depend only on the electron density and hydrogen-like argon profiles and the radiative recombination rate of H-like argon. We thus avoid the complexity inherent in other particle transport models that must take into account the radial profiles and ionization and recombination rates for all charge states of an ion present in the plasma.

Taking both D and $\partial n_{17}/\partial r$ to be independent of r over the limited region where the recombination steps occur we have

$$D = - \frac{1}{(r_2 - r_1) \frac{\partial n_{17}}{\partial r}} \int_{r_1}^{r_2} n_e(r) n_{17}(r) \alpha_{17}(r) r dr \quad .$$

Assuming a parabolic electron density profile and linear electron temperature profile we evaluate this expression numerically to obtain, for the hydrogen-like species of argon

$$D = (2.5 \pm 1.2) \times 10^4 \text{ cm}^2 \text{ sec}^{-1} .$$

This result may also be expressed in terms of a radial diffusion velocity, v_D :

$$v_D = (10 \pm 5) \text{ m/sec} .$$

This transport velocity was evaluated using the September 1978 data, a set of moderate density ($\langle n_e \rangle \sim 3 \times 10^{13} \text{ cm}^{-3}$) and temperature [$T_e(0) \sim 1.5 \text{ keV}$] discharges. In the region of interest the safety factor, q , is between 2 and 3. No significant MHD activity, such as sawtooth oscillations, that might enhance the transport was observed. The November 1976 data gave similar results. It is yet unknown how the diffusion coefficient scales with electron density and/or temperature, or how great an enhancement of the transport might result from non-diffusive processes. The particle confinement time as determined from the diffusion coefficient ($\tau_p \sim a^2/6D$, where a is the minor radius) is ~ 10 - 15 ms , which is, within a factor of two, the same as the bulk electron energy confinement time for these discharges. Recent measurements of the particle confinement from neutral injection⁴ and from spectroscopic investigation⁵ lead to comparable values.

Conclusion

This paper has presented evidence for the confirmation of the theory of recombination radiation; in particular, the observation of a recombination edge. The unusual size of this

edge has enabled us to determine a radially outward diffusion velocity for the hydrogen-like species of argon. It is clear that the technique of measuring transport from the recombination radiation of "long-lived" impurity ions ought to be equally useful for larger plasma confinement devices.

ACKNOWLEDGMENTS

The authors would like to thank W. Mycock, M. Perron and the PLT technical crew for their excellent assistance in the experiment. This project was supported by U. S. DOE Contract No. DE-AC02-76-CHO 3073.

REFERENCES

¹S. von Goeler, et al., "Thermal X-Ray Spectra and Impurities in the ST Tokamak," Nuc. Fus. 15, 301-311, 1975.

²A. L. Merts, R. D. Cowan, N. H. Magee, private communication of computer calculations.

³Ibid.

⁴H. Eubank, et al., "Neutral Beam-Heating Results from the Princeton Large Torus," Phys. Rev. Letters 43, pp. 270-274, 1979.

⁵K. Bol, et al., PPPL-1492, in Plasma Physics and Controlled Nuclear Fusion Research (Proceedings Seventh International Conference, Innsbruck, Austria, 1978) paper IAEA-CN-35/C-3, IAEA, Vienna (I,11-33) Dec. 1978.

FIGURE CAPTIONS

FIG. 1. Schematic of the experimental arrangement of the Pulse Height Analysis (PHA) system used to detect soft x-ray radiation on PLT. Four Si-Li detectors mounted on a movable arm to enable radial scans of the plasma yield line integrated spectra in four different energy regions. Count rates to the detectors are limited by a set of movable apertures and foils. The spectra are then processed by a PDP 10 computer, which corrects for foil attenuation, detector efficiency and aperture size, and overlaps the result into a single spectrum. The data may be Abel inverted to provide radial profiles of the electron temperature and impurity concentrations.

FIG. 2. Line integrated soft x-ray spectra obtained by the Pulse Height Analysis (PHA) system during special argon-seeded discharges on PLT. (Letters a and b refer respectively to measurements from November 6, 1976 and September 20, 1978). In figure 1a the spectra were taken over a period of 360 msec to 420 msec during the discharge; typical central electron temperatures and densities were 1.5 keV and $2.0 \times 10^{13} \text{ cm}^{-3}$. Resonant $K\alpha$ line emission of argon and iron is clearly visible in the plasma center. A large recombination edge at 4.1 keV (ξ is equivalent to the quantity $(\gamma - 1)$; see text) appears on the $r = 22.5 \text{ cm}$ spectrum, corresponding to an enhancement by a factor of one thousand over bremsstrahlung. In Figure 1b are presented some typical spectra at large minor radii from the 1978 discharges. The counting period extended from 300 to 500

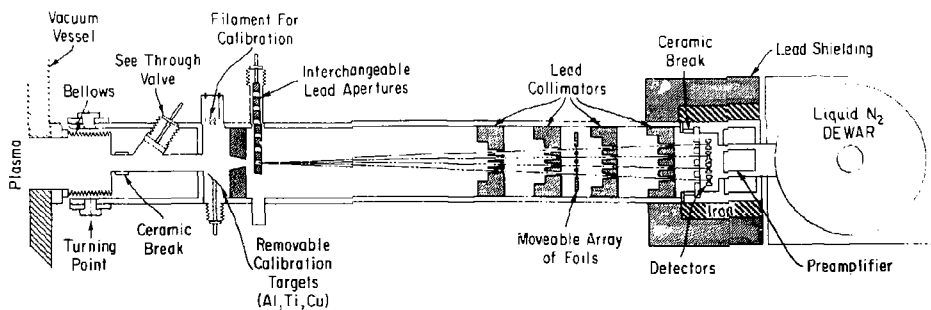
msec. Photon intensity (arbitrary units) is indicated on the ordinate; electron temperature and density profiles are presented in Figure 3. For each of the above spectra a titanium K α fluorescence line has been subtracted from the observed intensity (see text).

FIG. 3. Radial profiles of the electron density and temperature for the 1978 discharges. Density was determined by the microwave interferometer and the Thomson scattering diagnostics. The electron temperature was determined by Abel inversion of the line integrated soft x-ray spectra.

FIG. 4. Computer calculation of γ , defined as the enhancement over bremsstrahlung arising from radiative recombination with plasma ions, for various charge states of argon. Superimposed on these curves is the quantity γ_{eff} (equal to $\frac{\sum_i n_i \gamma_i}{\ln n_i}$) calculated under the assumption of corona equilibrium for the regions both before and after the 4.1 keV recombination edge.

FIG. 5. (a) Collisional ionization and, (b) net recombination cross sections of argon as a function of charge state, for several values of electron temperature.

FIG. 6. Radial profiles of the (a) total argon concentration, and (b) concentration of the hydrogen-like species for the 1978 discharges.



ELECTRONICS

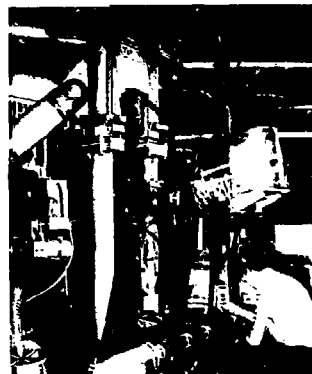
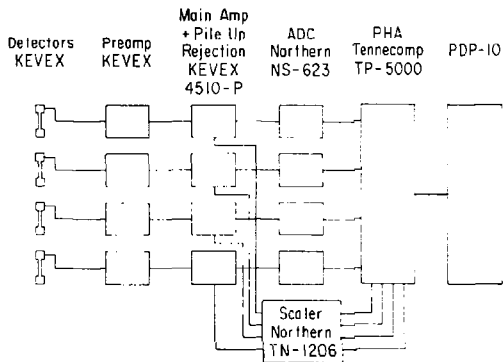


Fig. 1. (PPPL-773872)

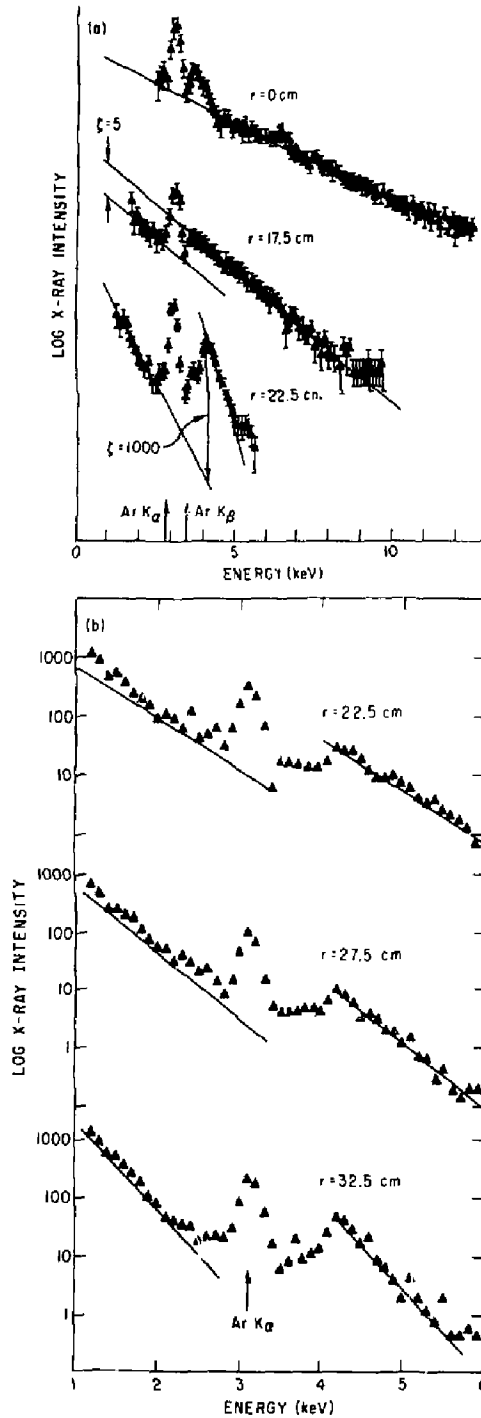
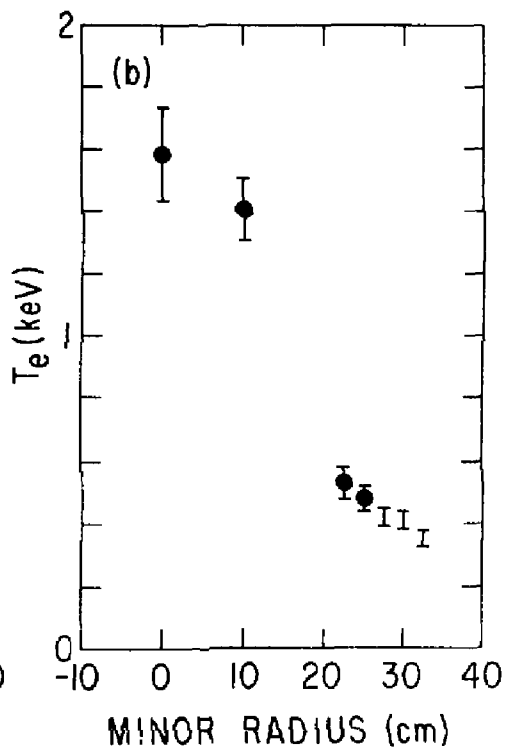
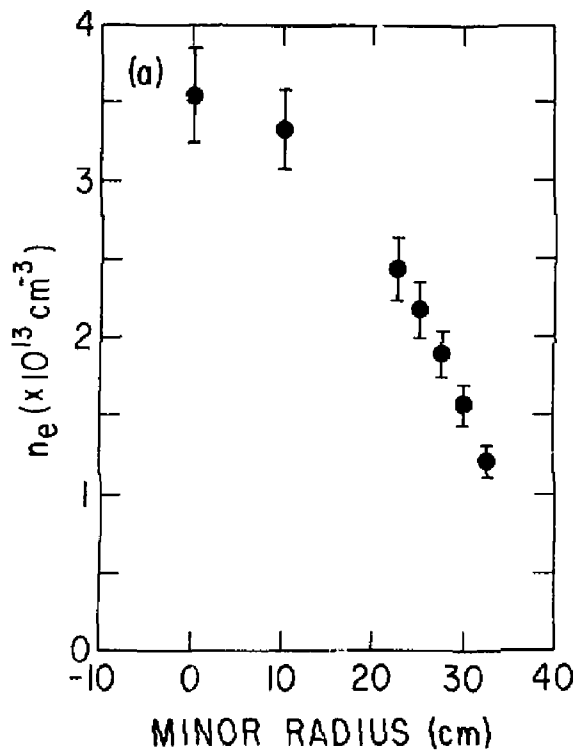


Fig. 2. (PPPL-803161)



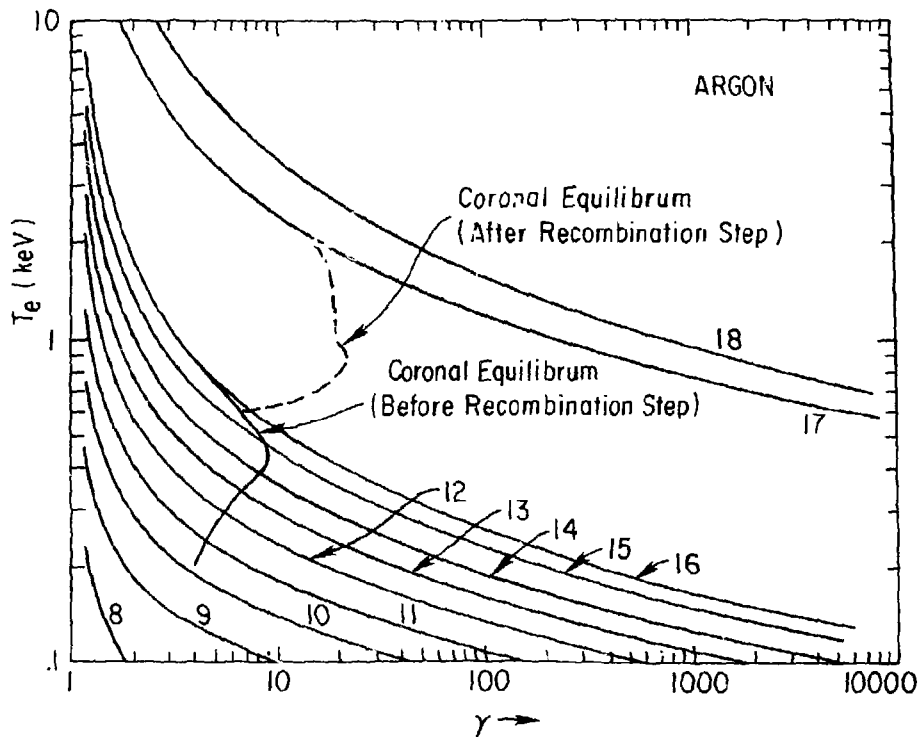


Fig. 4. (PPPL-783837)

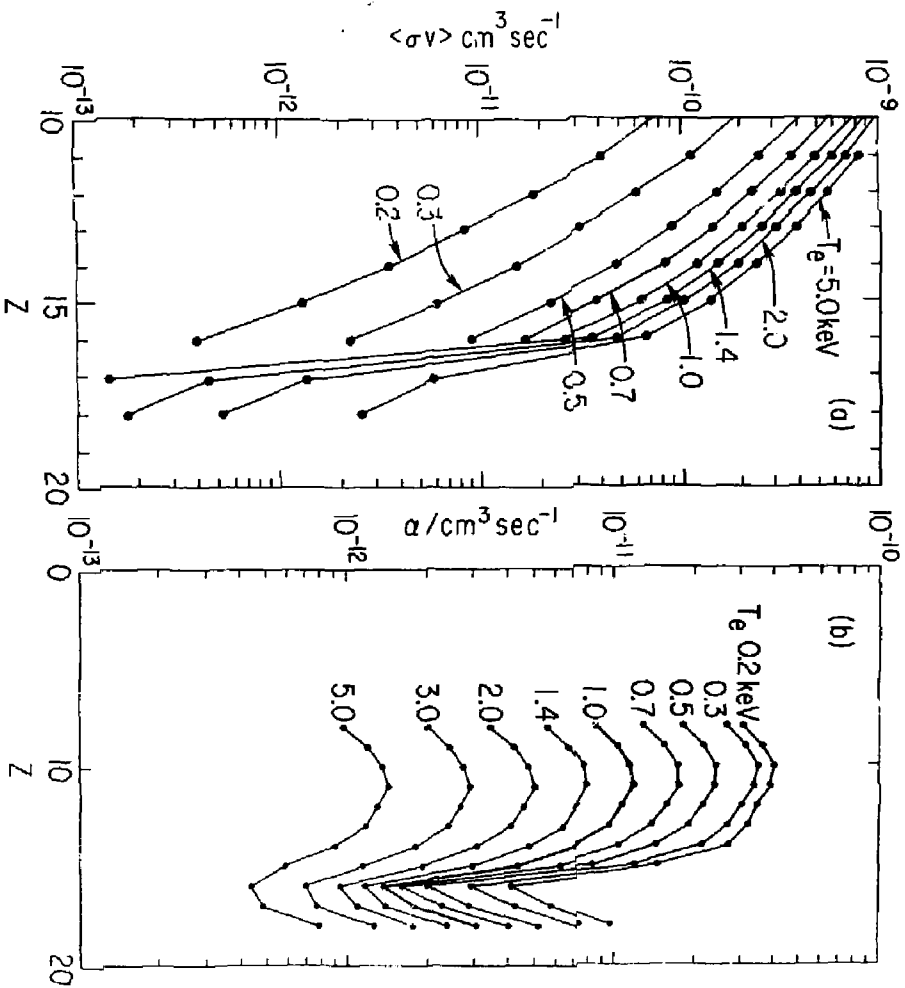
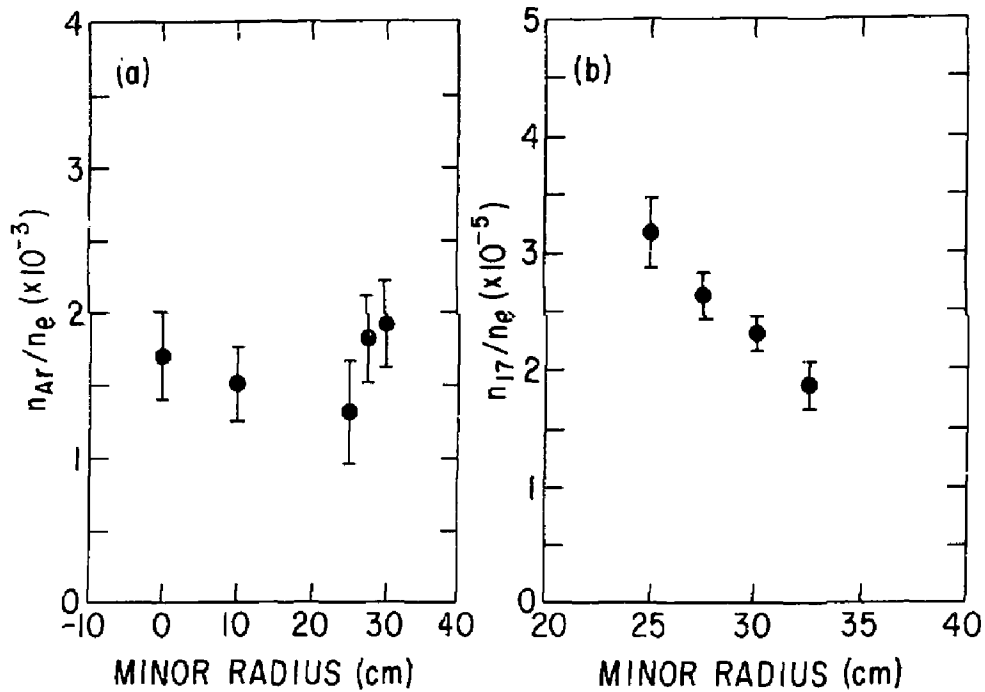


Fig. 5. (PPPL-803184)



EXTERNAL DISTRIBUTION IN ADDITION TO TIC UC-20

ALL CATEGORIES

- R. Askew, Auburn University, Alabama
 S. T. Wu, Univ. of Alabama
 Geophysical Institute, Univ. of Alaska
 G.L. Johnston, Sonoma State Univ, California
 H. H. Kuehl, Univ. of S. California
 Institute for Energy Studies, Stanford University
 H. D. Campbell, University of Florida
 N. L. Oleson, University of South Florida
 W. M. Stacey, Georgia Institute of Technology
 Benjamin Ma, Iowa State University
 Magne Kristiansen, Texas Tech. University
 W. L. Wiese, Nat'l Bureau of Standards, Wash., D.C.
 Australian National University, Canberra
 C.N. Watson-Munro, Univ. of Sydney, Australia
 F. Cap, Inst. for Theo. Physics, Austria
 Dr. M. Heindler, Institute for Theoretical Physics
 Technical University of Graz
 Ecole Royale Militaire, Bruxelles, Belgium
 D. Palmbo, C. European Comm. B-1949-Brussels
 P.H. Sakonak, Instituto de Fisica, Campinas, Brazil
 M.P. Bachynski, MPB Tech., Ste. Anne de Bellevue,
 Quebec, Canada
 C. R. James, University of Alberta, Canada
 T.W. Johnston, INRS-Energie, Vareennes, Quebec
 H. M. Skarsgard, Univ. of Saskatchewan, Canada
 Inst. of Physics, Academia Sinica, Peking,
 People's Republic of China
 Inst. of Plasma Physics, Hefei,
 Anhwei Province, People's Republic of China
 Library, Tsing Hua Univ., Peking, People's
 Republic of China
 Zhengwu Li, Southwestern Inst. of Phys., Leshan,
 Sichuan Province, People's Republic of China
 Librarian, Culham Laboratory, Abingdon, England (2)
 A.M. Dupas Library, C.E.N.-G, Grenoble, France
 Central Res. Inst. for Physics, Hungary
 S. K. Sharma, Univ. of Rajasthan, JAIPUR-8, India
 R. Shingal, Meerut College, India
 A.K. Sundaran, Phys. Res. Lab., India
 Biblioteca, Frascati, Italy
 Biblioteca, Milano, Italy
 G. Rostagni, Univ. Di Padova, Padova, Italy
 Preprint Library, Inst. de Fisica, Pisa, Italy
 Library, Plasma Physics Lab., Gokasho, Uji, Japan
 S. Mori, Japan Atomic Energy Res. Inst., Tokai-Mura
 Research Information Center, Nagoya Univ., Japan
 S. Shioda, Tokyo Inst. of Tech., Japan
 Inst. of Space & Aero. Sci., Univ. of Tokyo
 T. Uchida, Univ. of Tokyo, Japan
 H. Yamato, Toshiba R. & D. Center, Japan
 M. Yoshikawa, JAERI, Tokai Res. Est., Japan
 Dr. Tsuneo Nakakita, Toshiba Corporation,
 Kawasaki-Ku Kawasaki, 210 Japan
 N. Yajima, Kyushu Univ., Japan
 R. England, Univ. Nacional Auto-noma de Mexico
 B. S. Liley, Univ. of Waikato, New Zealand
 S. A. Moss, Saab Univas Norge, Norway
 J.A.C. Cabral, Univ. de Lisboa, Portugal
 O. Petrus, A.L.I. CUZA Univ., Romania
 J. de Villiers, Atomic Energy Bd., South Africa
 A. Maurech, Comisaria De La Energy y Recursos
 Minerales, Spain
 Library, Royal Institute of Technology, Sweden
 Cen. de Res. En Phys.Des Plasmas, Switzerland
 Librarian, Fom-Instituut Voor Plasma-Fysica,
 The Netherlands
- Bibliothek, Stuttgart, West Germany
 R.D. Buhler, Univ. of Stuttgart,
 West Germany
 Max-Planck-Inst. fur Plasmaphysik,
 W. Germany
 Nucl. Res. Estab., Julich, West Germany
 K. Schindler, Inst. Fur Theo. Physik,
 W. Germany
- EXPERIMENTAL
THEORETICAL
- M. H. Brennan, Flinders Univ. Australia
 H. Barnard, Univ. of British Columbia, Canada
 S. Sreenivasan, Univ. of Calgary, Canada
 J. Radet, C.E.N.-B.P., Fontenay-aux-Roses,
 France
 Prof. Schatzman, Observatoire de Nice,
 France
 S. C. Sharma, Univ. of Cape Coast, Ghana
 R. N. Ayyer, Laser Section, India
 B. Buti, Physical Res. Lab., India
 L. K. Chavda, S. Gujarat Univ. India
 I.M. Das, Banaras Hindu Univ., India
 S. Cuperman, Tel Aviv Univ., Israel
 E. Greenspan, Nur. Res. Center, Israel
 P. Rosenau, Israel Inst. of Tech., Israel
 Int'l. Center for Theo. Physics, Trieste, Italy
 I. Kawakami, Nihon University Japan
 T. Nakayama, Ritsumeikan Univ., Japan
 S. Nagao, Tohoku Univ., Japan
 J.I. Sakai, Toyama Univ., Japan
 S. Tjøtta, Univ. I Bergen, Norway
 M.A. Hellberg, Univ. of Natal, South Africa
 H. Wilhelmson, Chalmers Univ. of Tech.,
 Sweden
 Astro. Inst., Sonnenborgh Obs.,
 The Netherlands
 T. J. Boyd, Univ. College of North Wales
 K. Hubner, Univ. Heidelberg, W. Germany
 H. J. Kaeppler, Univ. of Stuttgart,
 West Germany
 K. H. Spatschek, Univ. Essen, West Germany
- EXPERIMENTAL
ENGINEERING
- B. Grek, Univ. du Quebec, Canada
 P. Lukac, Komenského Univ., Czechoslovakia
 G. Horikoshi, Nat'l Lab for High Energy Physics,
 Tsukuba-Gun, Japan
- EXPERIMENTAL
- F. J. Paoloni, Univ. of Wollongong, Australia
 J. Kistemaker, Fom Inst. for Atomic
 & Molec. Physics, The Netherlands
- THEORETICAL
- F. Verheest, Inst. Vor Theo. Mech., Belgium
 J. Teichmann, Univ. of Montreal, Canada
 T. Kahan, Univ. Paris VII, France
 R. K. Chhajlani, India
 S. K. Trehan, Panjab Univ., India
 T. Namikawa, Osaka City Univ., Japan
 H. Narumi, Univ. of Hiroshima, Japan
 Korea Atomic Energy Res. Inst., Korea
 E. T. Karlson, Uppsala Univ., Sweden
 L. Stenflo, Univ. of UMEA, Sweden
 J. R. Saraf, New Univ., United Kingdom